SIGNIFICANT ERROR PROPAGATION IN THE FINITE DIFFERENCE SOLUTION OF NON-LINEAR MAGNETOSTATIC PROBLEMS UTILIZING BOUNDARY CONDITION OF THE THIRD KIND

E. Afjei

Department of Electrical and Computer Engineering, Shahid Beheshti University
Tehran, Iran, afjei@yahoo.com

J. Rashed-Mohassel

Department of Electrical and Computer Engineering, University of Tehran
Tehran, Iran, jrashed@ut.ac.ir

M. H. Arbab

Department of Electrical and Computer Engineering, Shahid Beheshti University
Tehran, Iran, h-arab@hotmail.com

(Received: May 10, 2003 – Accepted in Revised Form: November 5, 2003)

Abstract This paper poses two magnetostatic problems in cylindrical coordinates with different permeabilities for each region. In the first problem the boundary condition of the second kind is used while in the second one, the boundary condition of the third kind is utilized. These problems are solved using the finite element and finite difference methods. In second problem, the results of the finite difference method show low magnetic vector potential as well as the magnetic field density when compared to the finite element results and in the linear case, to the analytical solution. This paper investigates the reason behind the low magnetostatic field computation in cylindrical coordinates using the finite difference method when boundary condition of the third kind is used. It then, presents a technique to overcome the problem of low magnetic field calculation using the finite difference method. The results obtained by the new technique are in close agreement with the finite element method as well as the analytical solution. Finally, it analyzes the possible source of error in modeling magnetostatic boundary conditions in finite difference formulation of vector Poisson or Laplace's equation in cylindrical coordinates.

Key Words Nonlinear Magnetic Field, Finite Difference, Finite Element, Electromagnetics

چکیده در این مقاله مساله مگنتواستاتیک استوانه ای با تراوایی متفاوت در دو ناحیه بررسی شده است. نشان داده شده است که با شرایط مرزی نوع دوم، پاسخ روش تفاضل محدود با پاسخ روش اجزاء محدود برای نواحی خطی و غیر خطی منحنی بی – اچ یکسان می باشد. اما در حالتی که شرط مرزی از نوع سوم است، پاسخ تفاوتهای محدود برای پتانسیل مغناطیسی و چگالی شار مغناطیسی در مقایسه با پاسخ اجزاء محدود، اختلاف قابل ملاحظه ای دارد و خطای موجود در روش تفاوت محدود زیاد است. در این مقاله، روشی برای اصلاح خطای یاد شده در میدان مغناطیسی ارائه شده است. نتایج این روش به پاسخ شیوه اجزای محدود بسیار نزدیک بوده و با جوابهای تحلیلی نیز مطابقت دارد. در نهایت منبع احتمالی خطا در مدلسازی شرایط مرزی مگنتواستاتیکی با فرمولبندی تفاوت محدود در معادله برداری پواسون و لاپلاس در مختصات استوانه ای تحلیل شده است.

1. INTRODUCTION

In this paper, the nonlinear magnetic field calculation has been investigated in two magnetostatic field problems applying the finite element and the finite difference techniques and then, the reason behind

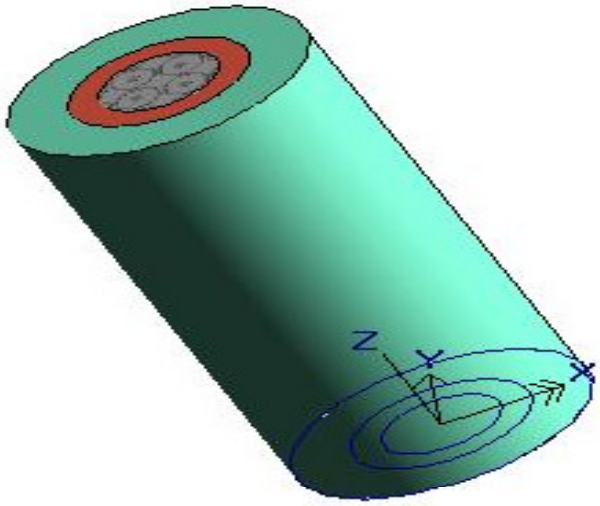

Figure 1. A cut view of the current carrying conductor and its surrounding.

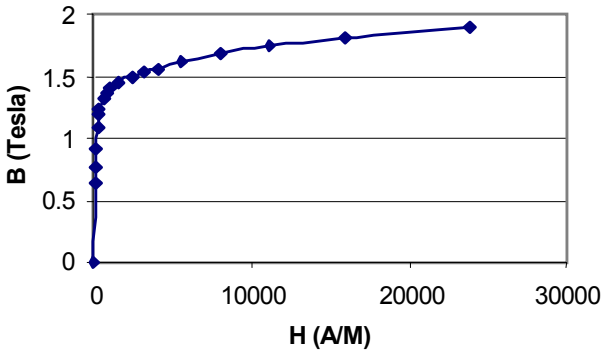

Figure 2. Static B-H curve for M-19 steel.

the inadequacy in the finite difference method is outlined. Afjei and Rashed have addressed the problem of inadequacies in finite difference solution of magnetic field in [1] for a linear case and outlined a procedure to fix this problem. The comparison of the first-order finite element and finite difference algorithms for the analysis of the magnetic field problems has been mentioned in [2-3]. The computation of magnetostatic field problems using the finite element technique as well as the finite difference method in Cartesian coordinates can be found immensely in the literature [4-7]. Now days computer packages using the finite element methods are available in the market which computes the magnetic field problems in all sorts of shape and geometry[8]. In this paper two case studies have been discussed. In the first case, a long current carrying conductor is considered with a relatively high permeable material (M-19: USS Transformer 72 ... 29 gage) surrounding the conductor where the boundary conditions are of the second kind. The second case considers a long core having the same high permeable material as problem one, with a coil wrapped around it. In this case the boundary conditions are of the third kind. These problems are solved by two different methods namely the finite element method and the finite difference technique and the results of both problems are then compared.

2. CALCULATION OF B-FIELD IN THREE CONCENTRIC CIRCLES

Consider a long current carrying conductor with a high permeable material surrounding the conductor. A cut view of the current carrying conductor and it's surrounding plus the corresponding cross section of the geometry is shown in Figure 1.

There are three concentric circles with different relative permeabilities. The center circle, which is a conductor, has a radius of r_a =1 Cm, the relative permeability of this region is one with a current density, J_z. Region two, which is made up of high permeable magnetic material (M-19: USS Transformer 72 ... 29 gage), has a radius of r_b = 3Cm. with the B-H curve shown in Figure 2.

Region 3, the surrounding medium, is the free space having a radius of r_c = 6 Cm.

In order to analyze the magnetic field in these regions, recognizing the low frequency nature of the problem, static field calculation has been performed. The static B-H curve has been broken into 5 different second order polynomials for the analysis. The corresponding vector potential equation is [9];

$$\nabla \times (\frac{\nabla \times A}{\mu_{(B)}}) = J \qquad (1)$$

where, $\mu_{(B)}$ is the permeability of the region at some

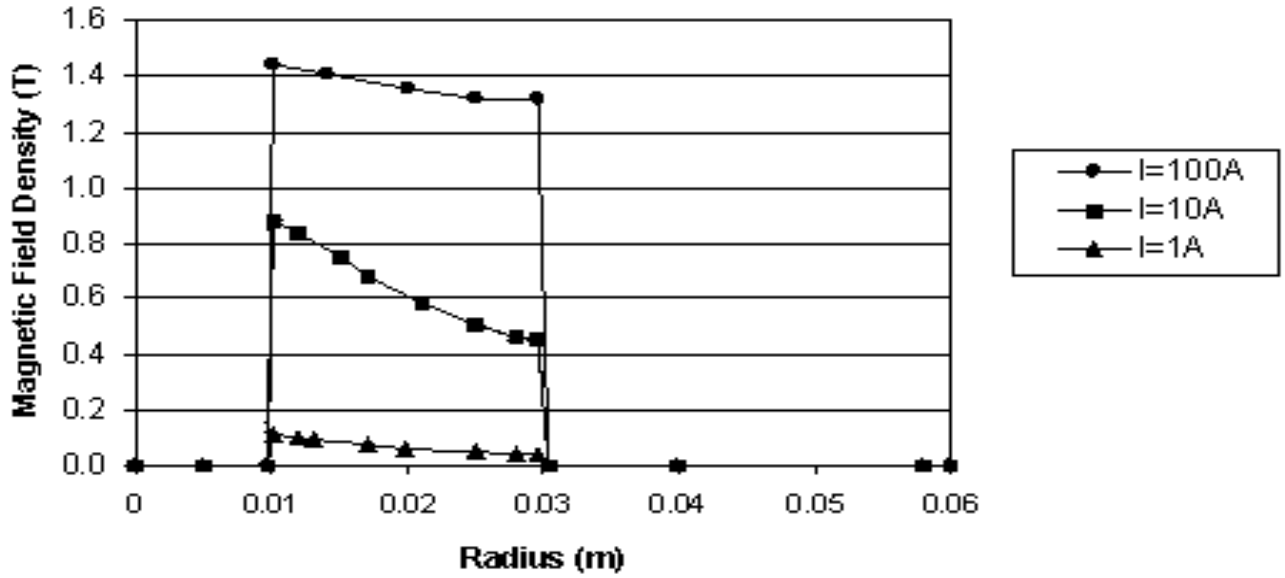

Figure 3. Magnetic field density versus radius for different current magnitudes (Finite Element).

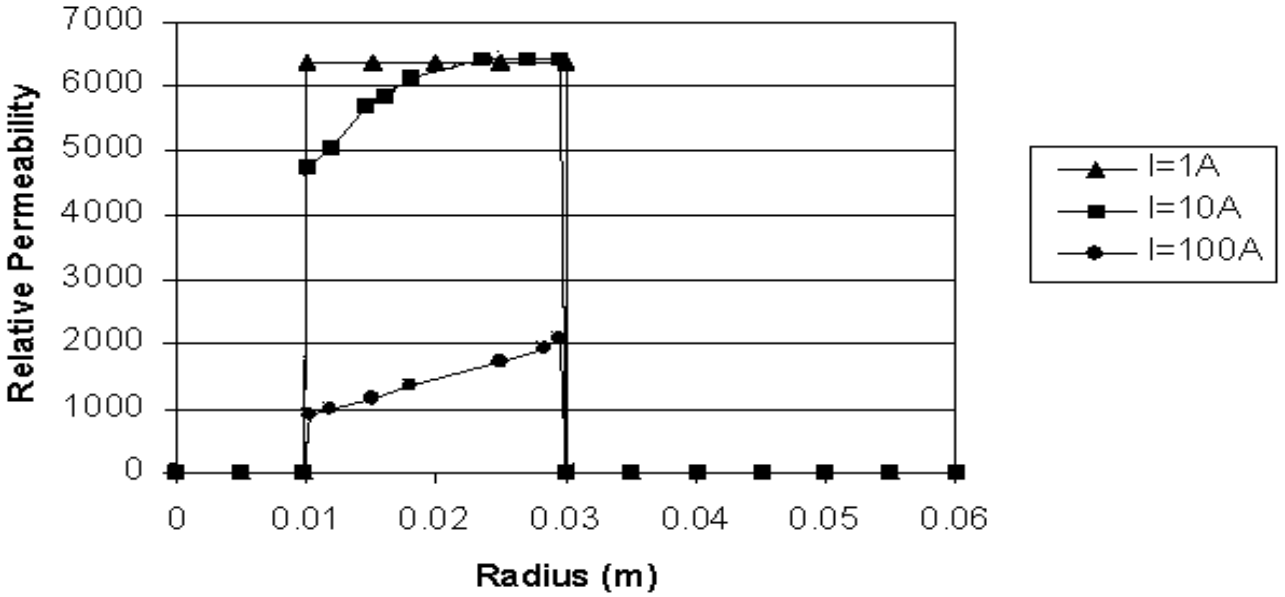

Figure 4. Relative permeability versus radius for different current magnitudes (Finite Element).

radius, r.

Due to symmetrical nature of the magnetic field, this problem can be simplified to a one-dimensional problem by realizing $\partial A_z / \partial \theta$ and $\partial A_z / \partial z$ are all zeroes.

Since the current is z-directed, Equation 1 becomes a scalar Poisson's equation in z-direction and, in cylindrical coordinate can be written as [10];

$$\frac{1}{r}\frac{\partial}{\partial r}\left(\frac{1}{\mu_B} r\left(\frac{\partial A_z}{\partial r}\right)\right) = -J \qquad (2)$$

We seek the solution to the Poisson's equation in region one and the Laplace's Equation is solved for regions two and three along with the appropriate boundary conditions. The appropriate boundary condition in terms of the vector potential results

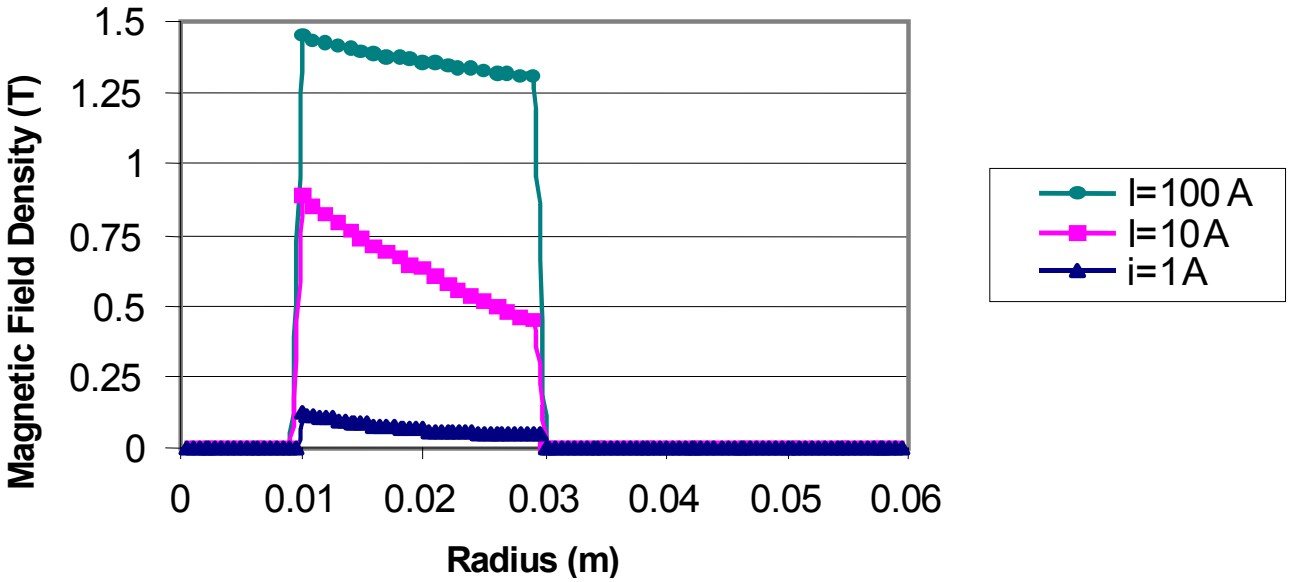

Figure 5. Magnetic field density vs. radius for different current magnitudes (Finite Difference).

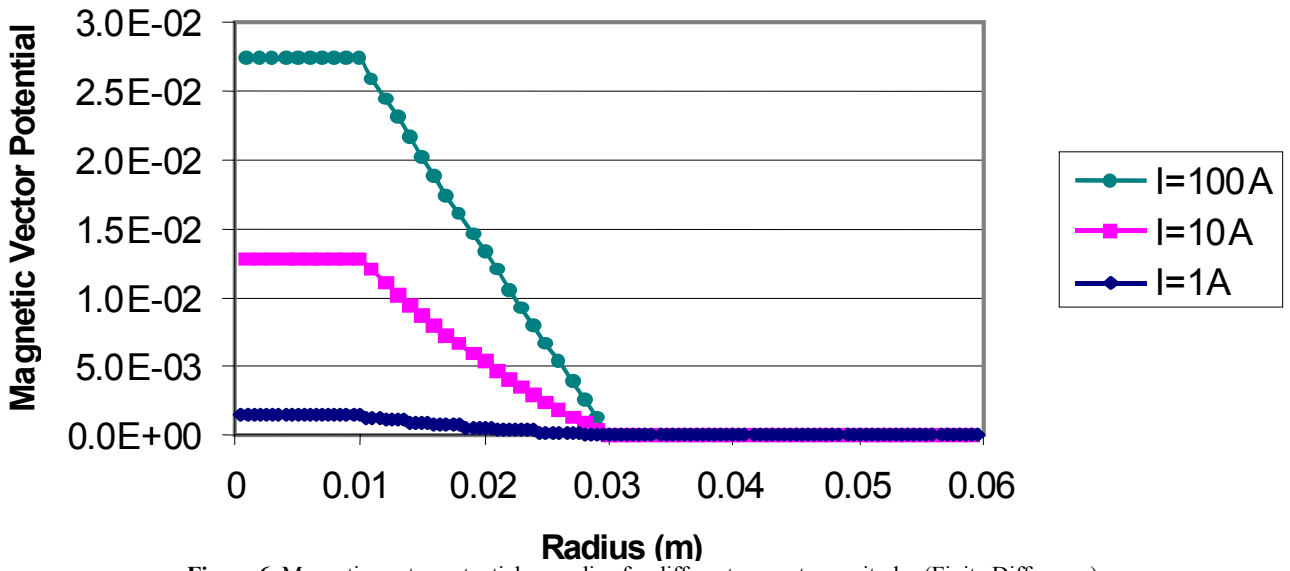

Figure 6. Magnetic vector potential vs. radius for different current magnitudes (Finite Difference).

from the continuity of the tangential component of magnetic field strength:

$$\frac{1}{\mu_1}\left(\frac{\partial A_z}{\partial r}\right)=\frac{1}{\mu_2}\left(\frac{\partial A_z}{\partial r}\right) \quad (3)$$

The above boundary condition is used at the interface of the first and the second regions, as well as the second and third regions. The outer boundary condition is

$$A_z I_{rmax} = 0 \quad (4)$$

This technique results in a solution for the vector potential, A_z. The magnetic flux density, B, then can be calculated by,

$$\overline{B} = \nabla \times \overline{A} \quad (5)$$

In the finite element technique, the variational method (Ritz) is employed to solve the cylindrical

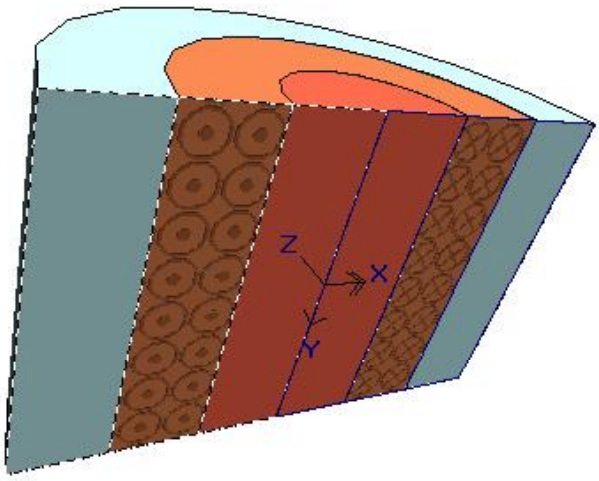

Figure 7. A cut view of the steel core with core wrapped around it and its surrounding.

form of vector Poisson's equation shown in 2. In the variational method, the solution to the partial differential Equation 2 obtained in r-direction by minimizing the following functional [10-11];

$$F(A)=\frac{1}{2}\int\left[\frac{r}{\mu_{(B)}}\left(\frac{dA}{dr}\right)^2\right]dr-\int rJ_zAdr \qquad (6)$$

The corresponding elemental stiffness matrix as well as the force vector for each element can be written as ;

$$K_{ij}=\int_{r_2}^{r_1}\frac{1}{\mu_{(B)}}\left[\frac{dN_i(r)}{dr}\frac{dN_j(r)}{dr}\right]rdr \qquad i,j=1,2 \quad (7)$$

$$F_i=\int_{r_2}^{r_1} rN_i(r)J_z\ dr \qquad i=1,2$$

In order to solve this problem, a constant $\mu_{(B)}$ from the linear part of the B-H curve is chosen for the core material and sets of simultaneous algebraic equations are formed by utilizing Equation 7 for all elements. The sets are then solved and from the solution new $\mu_{(B)}$ calculated. The new $\mu_{(B)}$ inserted into Equation 7 and other sets are formed, solved and a newer $\mu_{(B)}$ computed. This process repeated until the difference in $\mu_{(B)}$ from the last iteration with the one before that is less than some acceptable tolerance. It is noteworthy to mention that, the static B-H curve has been broken into 5 different second order polynomials for the analysis and used in the computation.

The plots of the magnetic field density, B, using the finite element technique as well as, the corresponding relative permeability for different current magnitudes from linear to fully non-linear cases are shown in Figure 3 and 4, respectively.

As seen from the above Figures, the plots are linear for 1A of current, then there is local saturation in the steel for 10A case, and finally for 100A study, the steel part of the medium has gone into full saturation. The results obtained for the magnetic field density and the magnetic vector potential from the finite difference method are shown in Figures 5 and 6, respectively.

A comparison of these results obtained by the finite difference and the finite element methods show very close agreement.

3. CALCULATION OF B-FIELD IN A LONG STATOR CORE

Consider a long cylindrical steel core with a coil wrapped around it. A cut view of the coil, direction of the current in the coil, and the it's surrounding is shown in Figure 7.

This problem consists of 3 regions. Region 1, which is made of high permeable magnetic material (M-19: USS Transformer 72 ... 29 gage), has a radius of r_a = 2Cm. with the B-H curve shown in Figure 2. Region 2 is a coil and has a current density only in θ direction (r_c =4 Cm, $J_\theta\neq0$, μ_r=1). Finally, region 3 is the surrounding medium, air and has a radius of r_b = 6 Cm. Since this problem is symmetric in θ-direction the vector potential has one component in this direction, and the problem can be solved in 1-dimension only. The cylindrical form of vector Poisson's equation, 1 is;

$$\frac{\partial}{\partial r}\left[\frac{1}{r\mu_{(B)}}\left(\frac{\partial}{\partial r}(rA_\theta)\right)\right]=-J_\theta \qquad (8)$$

with the following boundary conditions in terms of the vector potential in the cylindrical coordinate system;

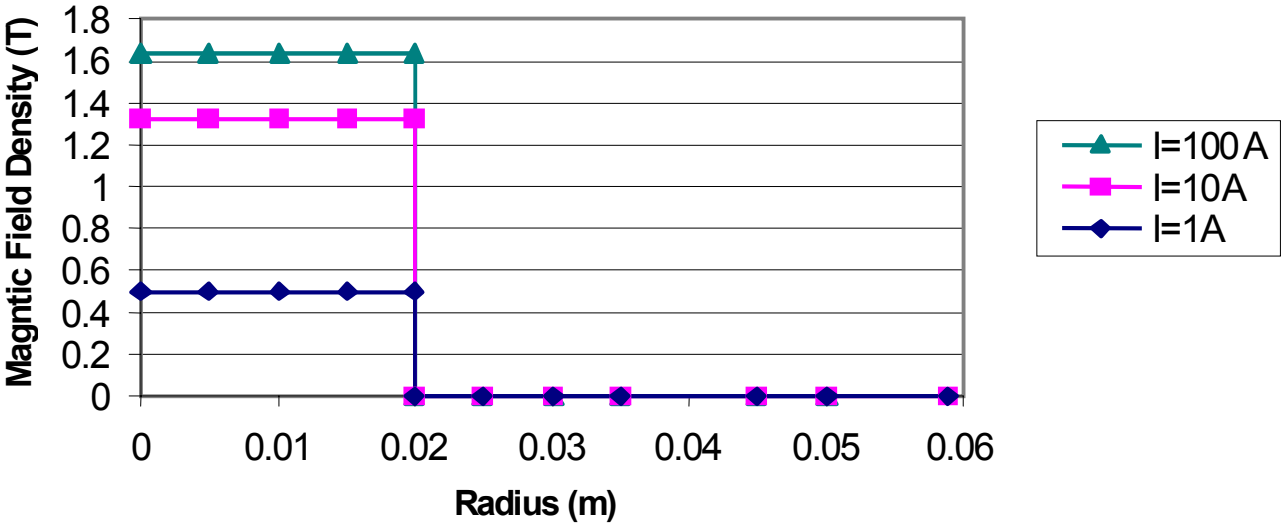

Figure 8. Magnetic field density versus radius for different current magnitudes (Finite Element).

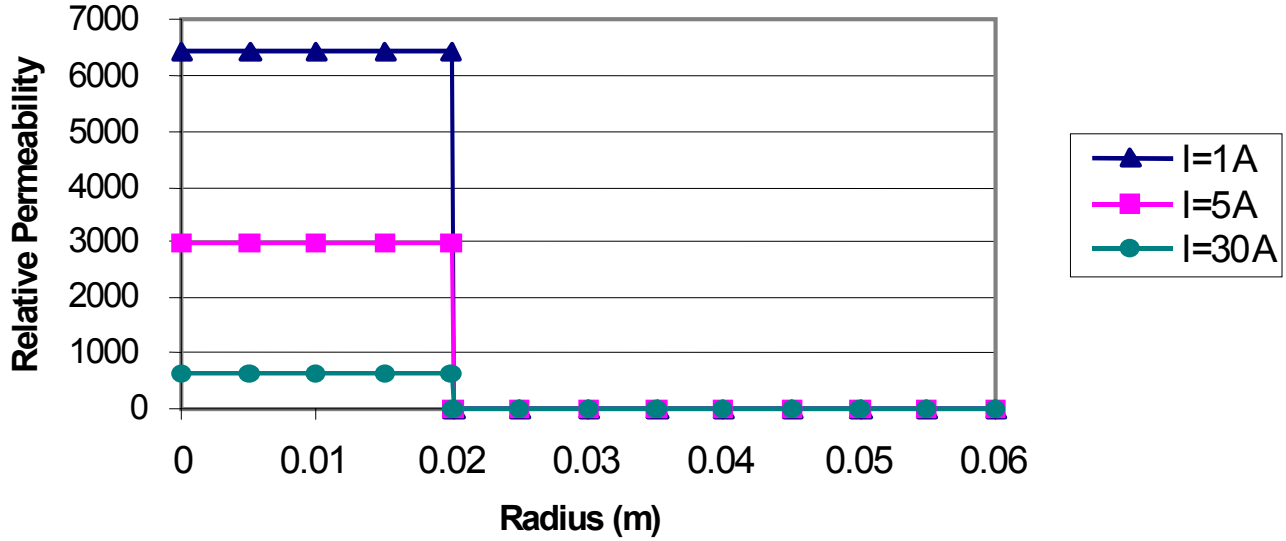

Figure 9. Relative permeability versus radius for different current magnitudes (Finite Element).

$$\frac{1}{\mu_1}\left(\frac{A_\theta}{r}+\frac{\partial A_\theta}{\partial r}\right)_1 = \frac{1}{\mu_2}\left(\frac{A_\theta}{r}+\frac{\partial A_\theta}{\partial r}\right)_2. \qquad (9)$$

The above boundary condition is known as the boundary condition of the third kind in which it involves the A_θ/r term. In the finite element technique, the variational method (Ritz) is employed to solve the cylindrical form of vector Poisson's equation shown in 8.

In the variational method, the solution to the partial differential Equation 8 obtained in r direction by minimizing the following functional [10-11];

$$F = \frac{1}{2}\int\left[\frac{1}{r\mu_{(B)}}\left(\frac{d(rA_\theta)}{dr}\right)^2\right]dr - \int rJ_\theta A dr \qquad (10)$$

The corresponding elemental stiffness matrix as well as the force vector for each element can be written as;

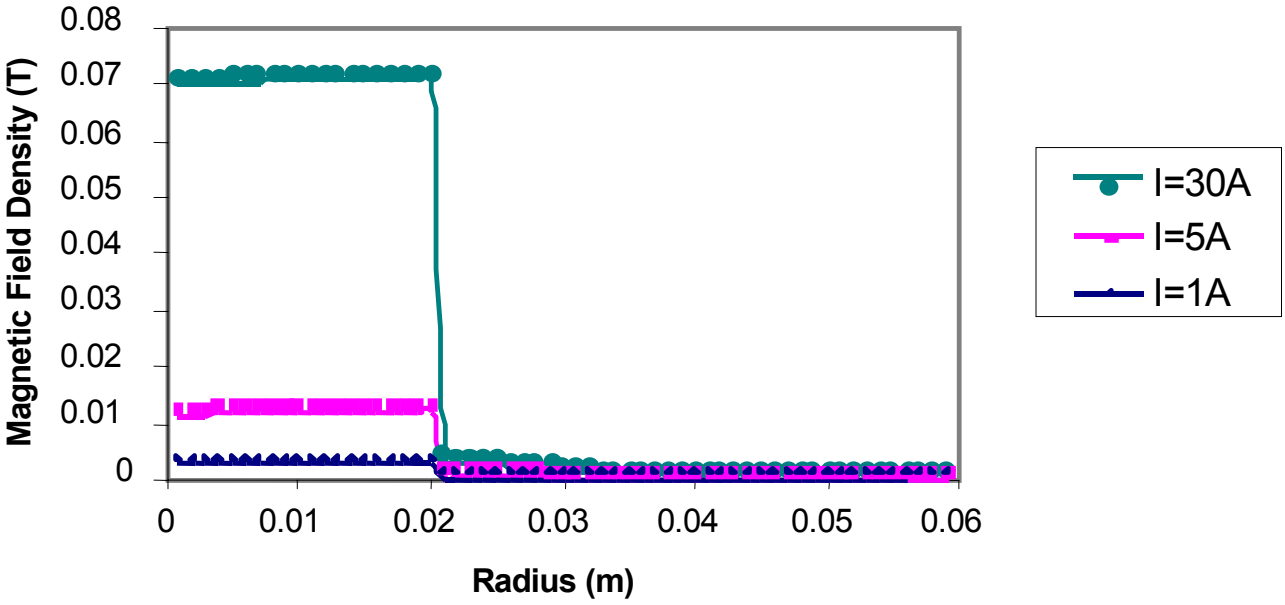

Figure 10. Magnetic field density versus radius (Finite difference).

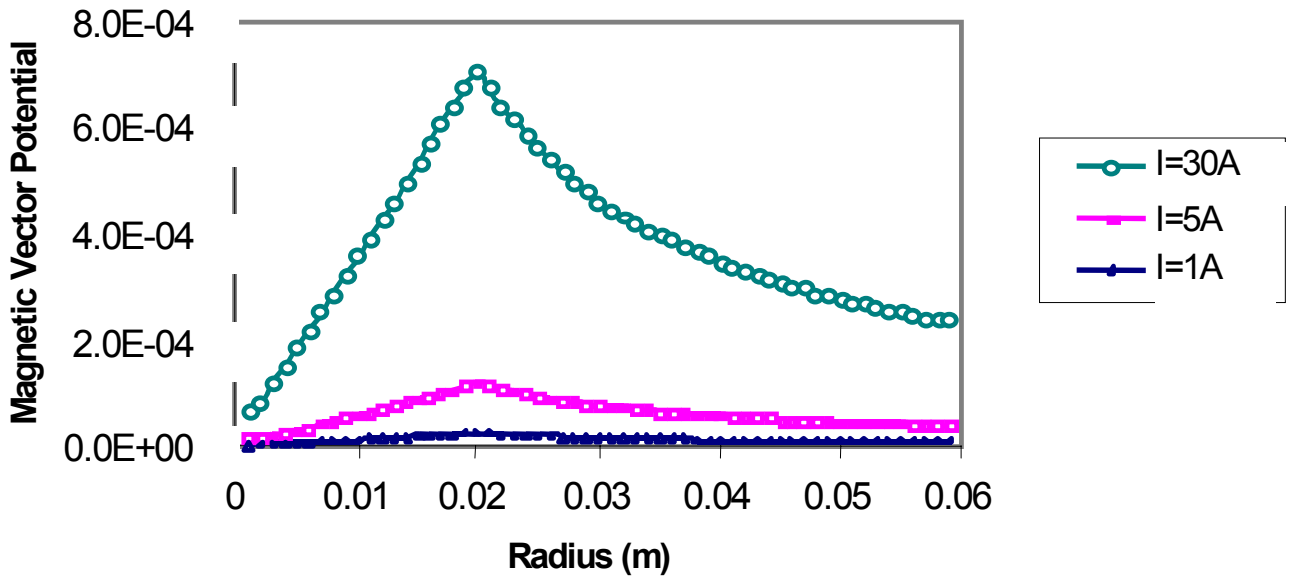

Figure 11. Magnetic vector potential versus radius.

$$K_{ij} = \int_{r_2}^{r_1} \frac{1}{r\mu_{(B)}} \left[\frac{dN_i(r)}{dr} \frac{dN_j(r)}{dr}\right] dr \qquad i, j = 1,2 \quad (11)$$

$$F_i = \int_{r2}^{r1} N_i(r) J_\theta \, dr \qquad i = 1,2$$

The magnetic field, B_z, is given by

$$B_z = \frac{A_\theta}{r} + \frac{\partial A_\theta}{\partial r} \quad (12)$$

The plots of the magnetic field density, B, using the finite element technique as well as, the corresponding relative permeability for different current magnitudes from linear to fully non-linear cases are shown in Figures 8 and 9, respectively.

As shown in the Figure 8 the magnetic field in

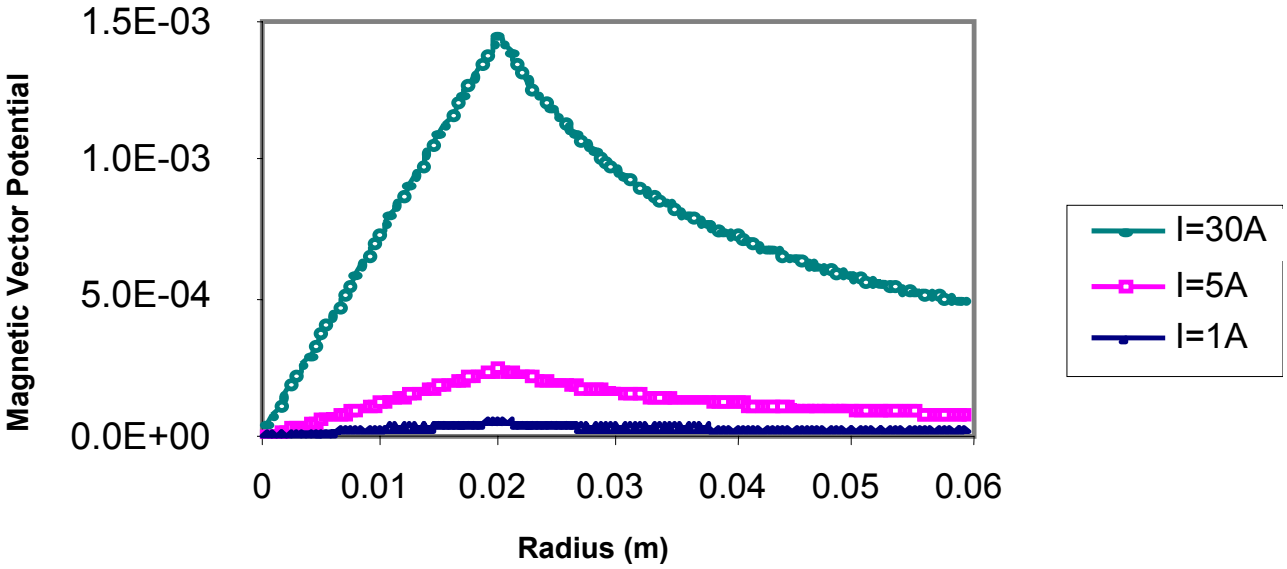

Figure 12. Magnetic field density versus radius for 120 points (Finite difference).

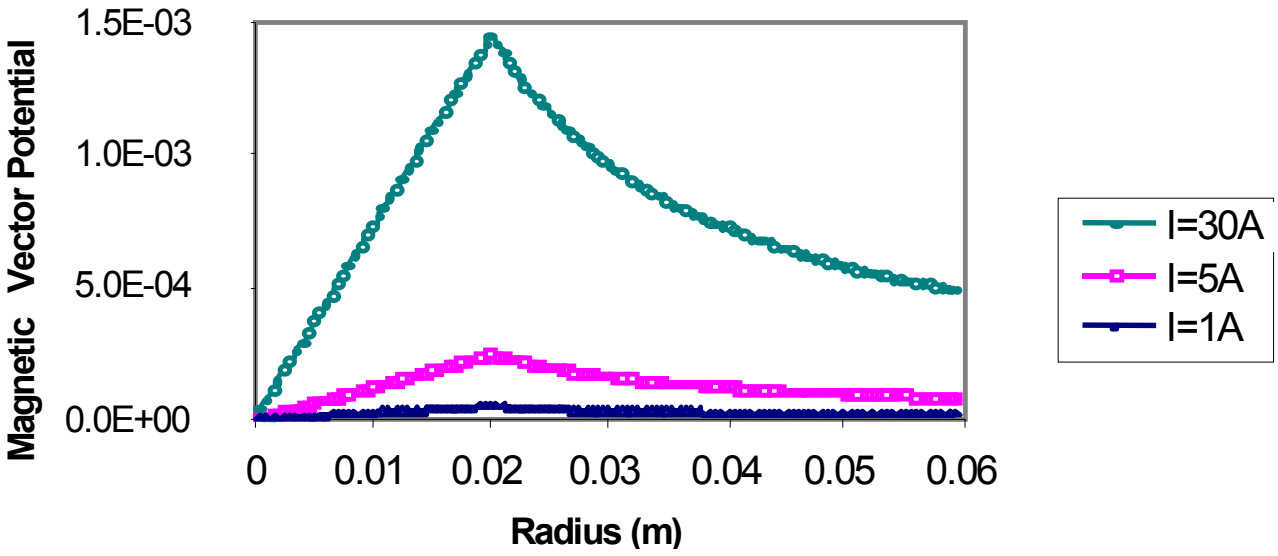

Figure 13. Magnetic vector potential versus radius for 120 points (Finite difference).

the core builds up to the maximum value and stays constant there. In Figure 9 the relative permeability has also stayed constant in the core and reduced to smaller values as the current magnitude increased. The number of turns is 5, therefore the corresponding current density for 1 A current is 3125 A/m2.

The result of magnetic field density and the magnetic vector potential using the finite difference technique for different current magnitudes and sixty nodal points are shown in Figures 10 and 11, respectively.

Comparing the plots in Figures 8 and 10 show different results for the finite element and finite difference solutions.

The discrepancy in the two results drastically increases when the relative permeability increases. It seems that the finite difference results are inaccurate when the relative permeability of the two media changes abruptly over the boundary. Now the number of grid points increased from 60

to 120 in the finite difference method and the magnetic field calculated again. Here are the results of magnetic field density and the magnetic vector potential.

The new calculation of the fields with 120 grid points shows closer results to the finite element method (but not accurate yet) when compared to the 60 grid points, therefore the error decreases as the grid point increases.

In order to verify the validity of the results, a comparison with the analytical solution should be performed.

4. ANALYTICAL SOLUTION

Since the permeability of the core stays at some constant value throughout the core region even in saturation then, Equation 8, can be transformed to a second order Cauchy-Euler equation and the analytical solution is

$$A_\theta = [\frac{\mu_{core}}{2}(R_c - R_a)\,J]\,r \quad \text{for} \quad 0 \le r \le R_a \qquad (13)$$

$$A_\theta = \left[\frac{\mu_{air} J R_c}{2}\right] r - \frac{\mu J r^2}{3} + \left[\frac{\mu_{core}}{2}(R_c - R_a)\,J\,R_a^{\,2} - \frac{\mu_{air} J R_c R_a^{\,2}}{2} + \frac{\mu_{coil} J R_a^{\,3}}{3}\right] r^{-1}$$

$$\text{for} \quad R_a \le r \le R_c$$

$$A_\theta = \left(\left[\frac{\mu_{air} J R_c}{2}\right] R_c^{\,2} - \left[\frac{\mu_{coil} J R_c^{\,3}}{3}\right] + \left[\frac{\mu_{core}}{2}(R_c - R_a)\,J\,R_a^{\,2} - \frac{\mu_{air}\, j R_c R_a^{\,2}}{2} + \frac{\mu_{coil}\, J R_a^{\,3}}{3}\right]\right) r^{-1}$$

$$\text{for} \quad r \ge r_c$$

where R_a is the radius of core, and R_c is the radius of coil.

The only problem here is that, the value of μ_{core} is not known and cannot be calculated analytically. The magnetic field is then obtained using

$$B_z = \frac{A_\theta}{r} + \frac{\partial A_\theta}{\partial r} \qquad (14)$$

can be written as;

$$\begin{aligned} B_z &= \mu_{core}(R_c - R_a)\,J \quad \text{for} \quad 0 \le r \le R_a \\ B_z &= \mu_{air}(R_c - r)\,J \quad \text{for} \quad R_a \le r \le R_c \\ B_z &= 0.0 \quad \text{for} \quad r \ge R_c \end{aligned} \qquad (15)$$

The plots of the magnetic vector potential and the magnetic field density cannot be shown unless the value of permeability of the core material is known but the general shape of the curves is the same as the finite element method for any relative permeability value chosen from Figure 9. In the linear case, the relative permeability of the core is known to be 6500. This value is substituted in the analytical solution; the shapes of the magnetic field density and the magnetic vector potential obtained are exactly the same as the finite element method but with a drastic drop in magnitude for the finite different technique. Hence, the numerical results obtained employing the finite difference method is not reliable.

In order to investigate the problem, the analytical solution is inserted in the finite difference representation of the boundary condition.

5. FINITE DIFFERENCE APPROXIMATION OF MAGNETOSTATIC FIELD

This section analyzes a possible source of error in modeling magnetostatic boundary conditions in a finite difference formulation of vector Poisson or Laplace Equation in cylindrical coordinates.

It was shown in section 3 that when magnetic fields are approximated from the vector potential using the first-order differences at the boundary, the results are in error. The error is proportional to the relative permeability of the two materials constituting the boundary. Only using an extremely fine mesh can minimize the error. The use of higher order differences can alleviate the problem, but yet the error remains proportional to relative permeability. An alternate formulation of the vector potential, in the one-dimensional case, is to make the error independent of the relative permeability of the two materials.

Now consider the problem in section 2, which requires the solution of the magnetic field density in and around an infinitely long solenoid. The interfacial

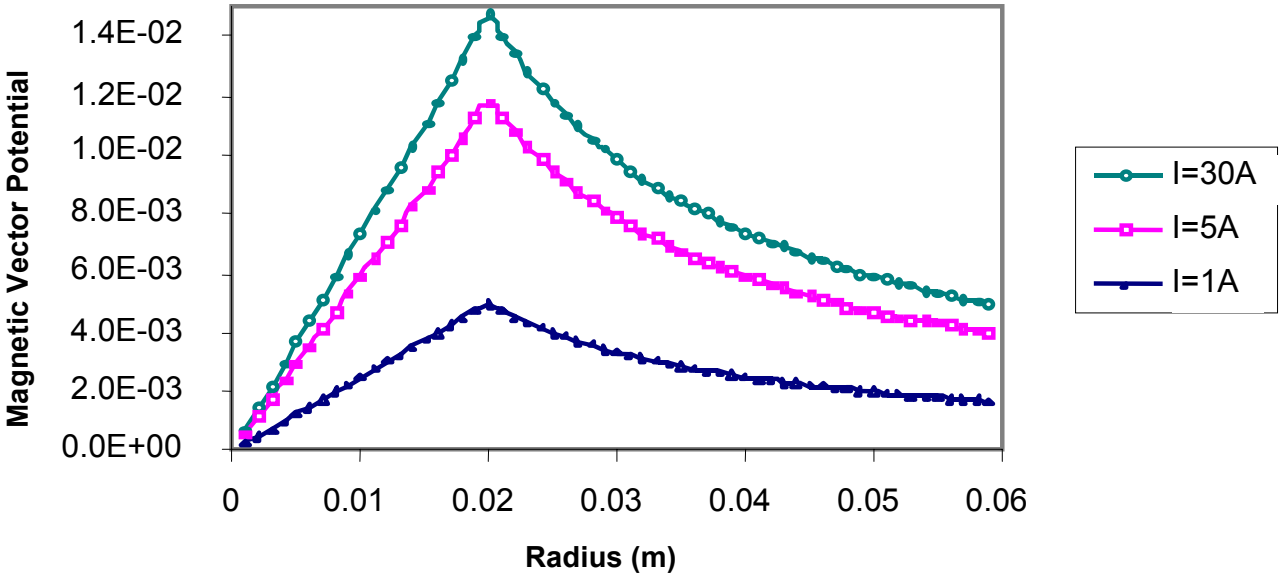

Figure 14. Magnetic vector potential versus radius (Finite difference).

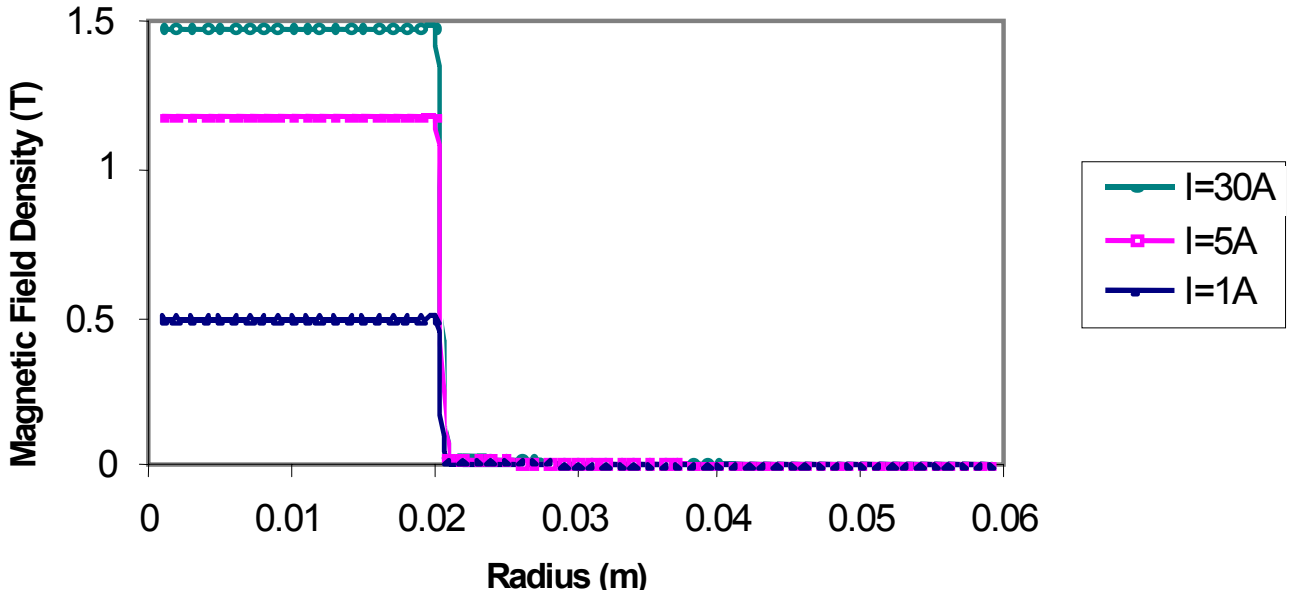

Figure 15. Magnetic Field Density Versus Radius.

condition between core and coil implies

$$\left[\frac{A_\theta}{r}+\frac{\partial A_\theta}{\partial r}\right]_{iron}=\mu_r\left[\frac{A_\theta}{r}+\frac{\partial A_\theta}{\partial r}\right]_{coil} \qquad (16)$$

at the boundary. Here $\mu_r = \mu_{core} / \mu_0$ is the relative permeability. In order to analyze the behavior of Equation 16, the discritization of the exact analytical solution at the boundary is examined. Without loss of generality, assume a constant value for the permeability of the magnetic material and a uniform grid size, d meter.

The (1/r) terms in A_θ do not contribute to flux density but arises from the requirement that A_θ is continuous. It should be noted that in the coil region the (1/r) term dominates since μ_{core} is large. Using first order differences on either side of the

boundary, the approximation to 16 becomes

$$\frac{A_\theta(r)}{r}+\frac{A_\theta(r)-A_\theta(r-d)}{d}= \mu_r\left(\frac{A_\theta}{r}+\frac{A_\theta(r+d)-A_\theta(r)}{d}\right) \quad (17)$$

Now substituting the analytical solution for A_θ in 17 and simplifying it, yields;

$$\mu_{core} \approx \mu_r[\mu_0 + k_1 d + k_2 \mu_{core}] \quad (18)$$

where k_1, and k_2 are constants.
In another words, expression in 18 can be written as;

$$\mu_{core} \approx \mu_{core} + \varepsilon \quad (19)$$

where, the error is directly proportional to μ_{core} and incremental distance d

It is observed that for a practical range of interest the error caused by high value of μ_r is substantial. Recognizing that the dominant (1/r) term is the one causing the error then, a new variable A'_θ is chosen such that $A'_\theta = r\, A_\theta$. The new formulation for the boundary condition and Laplace equations with this new variable are;

$$\left[\frac{\partial A'_\theta}{\partial r}\right]_{iron} = \mu_r \left[\frac{\partial A'_\theta}{\partial r}\right]_{coil} \quad (20)$$

$$\frac{\partial}{\partial r}\left[\frac{1}{r\mu_{(B)}}\left(\frac{\partial}{\partial r}(A'_\theta)\right)\right] = -J_\theta \quad (21)$$

The general solution to the Equation 21 employing boundary Equation 20 is

$$\begin{aligned} A'_\theta &= C_1 \mu_{core}\, r^2 && r \le R_a \\ A'_\theta &= C_2 \mu_0\, r^2 + (C_3 \mu_{core} - C_4 \mu_0) - C_5 \mu_0 r^3 && R_a \le r \le R_c \\ A'_\theta &= (C_6 \mu_{core} + C_7 \mu_0) && r \ge R_c . \end{aligned} \quad (22)$$

where C's are all constants
Using first order differences on either side of the boundary, the approximation to the new boundary Equation 20 is;

$$C_1 \mu_{core}\, r^2 - C_1 \mu_{core}(r-d)^2 = \mu_r [C_2\mu_0(r+d)^2 + C_5\mu_0(r+d)^3 - C_2\mu_0(r)^2 + C_5\mu_0(r)^3] \quad (23)$$

Where, in the right hand side of the Equation 23 the independency on the μ_{core} has been eliminated, therefore the dominant error in this problem is just a function of d.

$$\varepsilon = f(d) \quad (24)$$

As shown in the above Equations 23 and 24 the independency of the error on the μ_{core} has been eliminated. This approach should perform very well with a coarse grid too.

Comparing the new boundary condition with the previous one in 9, shows a simpler boundary equation and of the second kind. Equations 20 and 21 are solved using the finite difference method and results of the vector potential and magnetic field density are exactly the same as the one found by the finite element approach. These plots are shown in Figures 14 and 15, respectively.

As shown above, the problem of low magnetic field calculation is now fixed by changing the variable A_θ to the new variable A'_θ. The results obtained with the new variable using the finite difference method are the same as the result found by the finite element method.

6. CONCLUSIONS

In this paper two numerical techniques are used to calculate the non-linear magnetic field density for two different problems in cylindrical coordinates. It was found that, low magnetic field build up is being exhibited when the finite difference scheme in conjunction with the boundary condition of the third kind are used.

The problem of low magnetic field build up does not appear in the finite element method since the boundary conditions are satisfied naturally and are not forced, as in the finite difference technique.

It then continues with finding the cause error and hence demonstrating successfully a new method to change the boundary condition from the third kind to the second kind. Using this method, the independency of errors on relative permeability of high magnetic martial for the linear and non-linear B-H curve which caused the low field build up in finite difference technique has been eliminated. The results obtained are within less than 1% of the actual values.

7. REFRENCES

1. Afjei, E. and Rashed-Mohassel, J., "Inadequacies in Finite Difference Solution of Magnitostatic Problems", ***Iranian Journal of Science and Technology***, Transaction B, Vol. 25, No. B23, (2001), 533-541.
2. Fuchs, E. F. and McNaughton, G. A., "Comparison of First-Order Finite Difference and Finite Element Algorithms for The Analysis of Magnetic Fields. Part I: Theoretical Analysis", ***IEEE Transaction on Power Apparatus and System***, PAS- 101, No. 5, (May 1982), 1007-1015.
3. Fuchs, E. F. and McNaughton, G. A., "Comparison of First-Order Finite Difference and Finite Element Algorithms for The Analysis of Magnetic Fields. Part II: Theoretical Analysis", ***IEEE Transaction on Power Apparatus and System***, PAS-101, No. 5, (May 1982), 1027-1034.
4. Chari, M. V. K. et al., "Three Dimentional Magnitostatic Field Analysis Of Electric Machine", ***IEEE Transaction***, Vol. PAS-100, (1981), 4007-4019.
5. Csendes, Z. J. and Hoole, S. R. H., "Alternative Vector Potential Formulations for 3D-Magnetostatics", ***IEEE Transactions***, Vol. MAG-18, (1982), 367-372.
6. White, M. D., Chattot, J. J., "The Application of Finite Difference/Finite Volume Algorithm to Solve Maxwell's Equations in the Time Domain", ***Int. Journal of Comp. Fluid Dynamic***, (1995), 257-259.
7. Demerdash, N. A. N., Fouad, T. W. and Mohammed, F. A., "3-D Finite Element Vector Potential Formulation For Magnetic Fields in Electrical Apparatus", ***IEEE Transactions***, Vol. PAS-100, (1981), 4104-4111.
8. Magnet CAD Package, Infolytica Corp. Ltd., Montreal, Canada, (2001).
9. Chari, M. K. and Silvester, P. P., "Finite Element in Electrical and Magnetic Field Problems", New York, NY: John Wiley and Sons, (1984).
10. Afjei, E., "An Introduction to the Finite Element Method", Tehran, Iran, Ketabiran, (1998).
11. Jianming, J., "The Finite Element Method in Electromagnetics", New York, NY:John Wiley and Sons,(1993).